Weather and Climate Extremes 42 (2023) 100632

Contents lists available at ScienceDirect

Weather and Climate Extremes

journal homepage: www.elsevier.com/locate/wace

Drought-heatwave compound events are stronger in drylands

Chuan Wang [a,b], Zhi Li [a,*], Yaning Chen [a], Lin Ouyang [c], Yupeng Li [a], Fan Sun [a,b], Yongchang Liu [a,b], Jianyu Zhu [a,b]

[a] State Key Laboratory of Desert and Oasis Ecology, Key Laboratory of Ecological Safety and Sustainable Development in Arid Lands, Xinjiang Institute of Ecology and Geography, Chinese Academy of Sciences, Urumqi, 830011, China
[b] University of Chinese Academy of Sciences, Beijing, 100049, China
[c] School of Atmospheric Sciences, Nanjing University of Information Science and Technology, Nanjing, 210044, China

ARTICLE INFO

Keywords:
Extremes
Heatwave
Droughts
Compound events
Drylands

ABSTRACT

Climate change is exacerbating the occurrence of compound droughts and heatwaves (CDHWs), which pose a serious threat to human health and socio-economic development. Using daily maximum temperature (Tmax) and monthly self-calibrating Palmer drought severity index (sc-PDSI) dataset, the evolution patterns of CDHWs and compound wet-heatwave events, the dominant drivers and the relative contributions of droughts and heatwaves in the drylands and humid areas from 1961 to 2020 were compared and analyzed. The results show that the CDHWs are stronger in drylands than in humid areas, the growth rate of CDHWs in drylands was almost twice that of the humid areas, the CDHWs are greater than the multi-year average intensity of compound wet-heatwave events by up to 2.4 times. Moreover, CDHWs has increased significantly from the past period (1961–1990) to the recent warm period (1991–2020), and the heatwave threshold has increased by about 5 °C. In most drylands, the contribution of heatwaves to CDHWs dominates, whereas in humid areas, the droughts contribution to CDHWs does. The compounding effects of droughts and heatwaves may exacerbate the severity of CDHWs regionally and are most pronounced in drylands, taking into account optimal lags. The study findings could provide scientific and technological support to actively address global climate change risks.

1. Introduction

The world is currently experiencing climate change characterized by warming, and any continued warming in the future will lead to more frequent and severe extreme events (Zscheischler et al., 2018, 2020). These events primarily include floods, droughts, and heatwaves (Xu et al., 2019; Sutanto et al., 2020; Wang et al., 2022). Extreme weather events are more sensitive to climate change, showing obvious sudden onset and often difficult to predict and prevent. Compound events may have more severe impacts on the natural environment and human society than single extreme weather events (Barichivich et al., 2019; Brás et al., 2021). When droughts and heatwaves occur together, they are called compound droughts and heatwaves (CDHWs). These events can have a profound impact on agricultural output and our natural environment. For example, the probability of corn yield reduction increases by about 20% when droughts or extreme heat transitions to CDHWs (Feng et al., 2019). In Southern and Eastern Europe, tree mortality was found to be associated with CDHWs, which may have been exacerbated by a gradual and steady increase in summer temperatures and vapor pressure deficit (VPD), which is expected to lead to higher tree mortality in the future (Gazol and Julio Camarero, 2022). A positive trend of increasing frequency, intensity, and duration of CDHWs has been found in most regions of the world and is most pronounced in Australia, Asia, and Europe (Mukherjee and Mishra, 2021; Shi et al., 2021; Wu et al., 2021).

Given the enormous impact of extreme compound events, CDHWs have received a great deal of attention from the scientific community in recent years (Bevacqua et al., 2022; Feng et al., 2019; Perkins-Kirkpatrick and Lewis, 2020). One study found a constraining effect of average precipitation trends on future CDHWs. This is due to the fact that the magnitude of localized warming is large enough that future droughts are more likely to coincide with extreme thermal events, exacerbating the intensity of CDHWs (Bevacqua et al., 2022). The Arctic amplification effect refers to the fact that temperatures in the Arctic are rising faster than the global average in the context of global warming (Rantanen et al., 2022). Similarly, a study exploring the spatial and temporal

* Corresponding author.
E-mail address: liz@ms.xjb.ac.cn (Z. Li).

https://doi.org/10.1016/j.wace.2023.100632
Received 21 March 2023; Received in revised form 16 November 2023; Accepted 17 November 2023
Available online 22 November 2023
2212-0947/© 2023 The Authors. Published by Elsevier B.V. This is an open access article under the CC BY-NC-ND license (http://creativecommons.org/licenses/by-nc-nd/4.0/).

variability of CDHW events from 1983 to 2016 found that CDHWs have a significant global impact, occurring in an asymmetric spatial pattern, with greater intensity in the Northern Hemisphere, which corresponds to Arctic amplification (Mukherjee and Mishra, 2021). Some researchers defined compound agricultural droughts and hot events (CADHEs) and analyzed their variability and drivers, and found that CADHEs tended to increase in all regions except central China, where the relative contribution of temperature to CDHWs was high, and that the increase in CADHEs in northeastern China underscored the importance of soil moisture-temperature dependence in the contribution to the variability of the compound events (Zhang et al., 2022). A Bayesian approach was utilized to identify the climate regions most vulnerable to the impact of heatwaves being exacerbated by droughts. The findings suggest that restricting global warming to 1.5 °C could significantly alleviate CDHWs in these identified regions (Mukherjee et al., 2022). CDHWs also pose a serious threat to vegetation and socio-economic systems and will further affect the capacity of terrestrial carbon sinks (Yin et al., 2023; Zhou et al., 2019).

Common compound extreme events can be broadly classified into four categories: pre-impact types, such as spring droughts that exacerbate summer heatwave; simultaneous types, such as severe heatwave and drought events; sequential types, such as sustained daytime and nighttime heatwave events; and spatially linked, multiple event types, which have common impact effects in space (Zscheischler et al., 2020). CDHWs may be closely related to land atmospheric feedback, internal forcings (ENSO), changes in subsurface conditions due to anthropogenic activities, and hydrologic processes. Land atmospheric feedback affects soil moisture and vegetation cover. ENSO may affect soil moisture and vegetation cover by altering the atmospheric circulation pattern, anthropogenic activities alter the surface heat and moisture characteristics, and hydrologic processes, especially surface runoff and evapotranspiration, and changes in these conditions may cause changes in CDHWs (Domeisen et al., 2022; Hao, 2022; Hao and Singh, 2020). Researchers used return period and joint probability methods to study the changes and driving factors of agricultural compound dry heat events in eastern China, highlighting that the enhanced soil moisture-temperature dependence plays an important role in the increase of compound events (Zhang et al., 2022). Some researchers have also assessed the changes of dry-heat compound events in China by defining Standardized Compound Event Indicator (SCEI) and Standardized Dry Hot Index (SDHI) based on precipitation and temperature on a monthly scale. The study found that the severity of dry-heat compound events increased significantly in most regions of China, and that temperature contributed more to the dry-heat compound events (Wu et al., 2020a). Despite extensive research on CDHWs, the differences in CDHWs between drylands and humid areas and the factors that dominate them are not known (Le et al., 2020; Pyrgou et al., 2020; Reddy et al., 2022).

The expansion of drylands is on an accelerating trend and is expected to reach half of the land area by the end of the century (Huang et al., 2016). Increased warming could lead to more extreme events as droughts increase (Li et al., 2017), Attention to the differences between drylands and humid areas appears to be crucial. Furthermore, research on the occurrence and evolution of CDHWs in drylands can explore how these areas cope with climate change while still promoting ecological security as well as sustainable economic and social development in the affected regions (An et al., 2021). Grasping the characteristics of changes in extreme compound events will help provide a scientific basis for disaster prevention and mitigation in response to climate change (Hoover et al., 2022; Ridder et al., 2022; Zhou and Yuan, 2022). In summary, there is an urgent need to understand the changing character of CDHWs. The potential for CDHWs to cause serious impacts should be addressed in a rational manner. This paper uses the daily maximum temperature (Tmax) and monthly-scale self-calibrated Palmer Drought Severity Index (sc-PDSI) datasets. Unites multiple research indicators of CDHWs, based on their occurrence in drylands and humid areas globally from 1961 to 2020. It will focus on the following three main points: (1) the evolution pattern of CDHWs under different zonation conditions, emphasizing the difference in the occurrence of CDHWs in drylands and humid areas; (2) CDHWs and compound wet-heatwave events are compared. The transition of CDHWs and compound wet-heatwave events from the past period (1961–1990) to the recent warm period (1991–2020) is also investigated; and (3) determining the relative contribution of droughts and heatwaves to CDHWs and their compound on the difference areas.

2. Materials and methods

2.1. Data source

The precipitation and potential evapotranspiration data required for aridity index (AI) calculations were obtained from the University of East Anglia Climate Research Center (CRU) of TS v4.05 dataset (1961–2020) (https://crudata.uea.ac.uk/cru/data/). Potential evaporation was calculated using the FAO Penman Monteith formula, as the Thornthwaite equation only considers temperature (Harris et al., 2020). The AI is defined as the ratio of precipitation to potential evapotranspiration (Li et al., 2019) and can be used to classify climates in different regions (Baltas, 2007). Fig. 1(a) illustrates the world divided into arid and humid areas, with the arid area further divided into eight global arid areas. Due to the absence of CDHW results in hyper-arid areas, we masked CDHWs and retained only four types: arid, semi-arid, dry--semihumid, and humid areas. The results of this division are consistent with the research results of Huang et al. (2016).

Using daily Tmax data from the Berkeley Earth Surface Temperature(project (http://berkeleyearth.org/data/), the resolution of the data was 1°, a preliminary pooled dataset was created by merging 1.6 billion temperature reports from 16 existing data archives (Rohde and Hausfather, 2020). We also used the 1981–2020 Climate Prediction Center (CPC) Tmax data (https://www.esrl.noaa.gov/psd/; spatial resolution of 0.25°) . Comparison of CPC data and Berkeley data for CDHWs. Self-calibrating Palmer Drought Severity Index (sc-PDSI) from Climate Research Unit (CRU) (https://crudata.uea.ac.uk/cru/data/drought/) (Barichivich et al., 2019), the resolution of the data was 0.5°. The sc-PDSI is based on a monthly scale and includes methods for dynamically calculating constants. It uses characteristics of each station location and can be applied to meteorological, agricultural and hydrological drought situations (Wells et al., 2004). In order to ensure the consistency of temperature data sources in heatwaves and droughts, the analysis obtained a correlation coefficient of 0.99 between Berkeley_Tmax and CRU_Tmax, which basically avoids the error of CDHWs caused by inconsistency of temperature data sources (Fig. S1). In order to calculate CDHWs, sc-PDSI was interpolated to a 1° spatial resolution by bilinear interpolation.

2.2. Methods

2.2.1. Define heatwave events and drought/wet events

Relative threshold methods suitable for large regional scales are often used to calculate heatwaves. This approach, in which heatwave occurrence is confirmed when the daily maximum temperature exceeds the 90% threshold for at least three consecutive days, also has good applicability of its relative threshold for various climate areas (Mukherjee and Mishra, 2021; Perkins-Kirkpatrick and Lewis, 2020). We calculated different thresholds for all grid points in the world in the time direction. The thresholds were defined based on 60 temperature samples corresponding to the highest temperature for each grid point every day from 1961 to 2020. Finally, the daily maximum temperature and the different thresholds of grid points were calculated in order to compare and judge whether a heatwave has occurred. If the value of the sc-PDSI reaches the threshold of drought/wet, we consider that a drought/wet event has occurred, That means sc-PDSI < -1 is defined as a drought event, and sc-PDSI>1 is defined as a wet event (Maule et al., 2013).

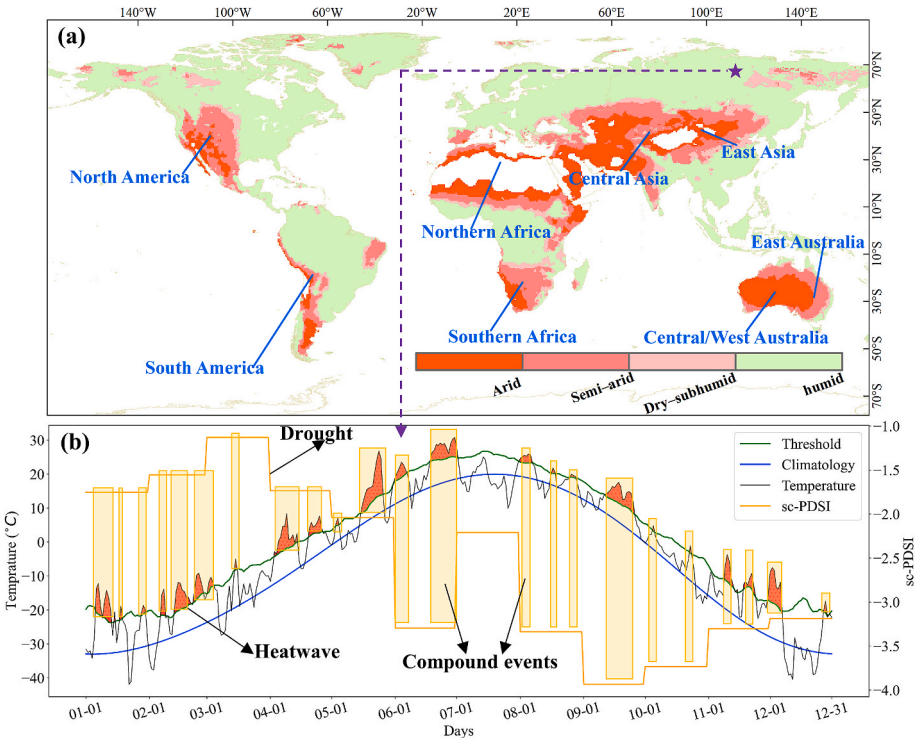

Fig. 1. (a) Study area: drylands and humid areas based on aridity index (AI) classification, (b) schematic diagram of the mechanism of drought-heatwave compound events (orange shading represents the occurrence of CDHWs events, for the year 2020, 67°N, 110°E and marked with a purple pentagram in Fig. 1a). (For interpretation of the references to colour in this figure legend, the reader is referred to the Web version of this article.)

2.2.2. Define CDHWs and compound wet-heatwave events

CDHWs are derived based on the intersection of drought and heatwave information. Firstly, the daily-scale temperature data are sorted in the time direction to identify heatwaves, different heatwave indicators are then defined based on heatwaves, including six indicators of frequency, duration and intensity (Table 1), and the conversion of daily-scale heatwave characteristics to monthly scales is based on the frequency, duration and intensity of occurrence in each month, and finally combined with the monthly-scale drought indicators. In general, heatwaves that occur under drought conditions are considered a CDHW event (Hao and Singh, 2020; Sutanto et al., 2020). Among them, multiple heatwaves within a drought event correspond to multiple CDHWs (Fig. 1(b)), which further represents the occurrence process and duration of CDHWs.

The total frequency of CDHWs (DHF) is defined as the total frequency of CDHWs in a month/year, and the maximum duration of CDHWs in days (DHD) is defined as the maximum number of days when a CDHW occurs in a month/year. The total occurrence days of CDHWs (DHO) is defined as the sum of the total occurrence days of CDHWs in a year/month. The average magnitude of CDHWs (DHM) is defined as the ratio of the DHF and the sum of drought days in a month/year, namely DHF/drought. Introduce cumulative heat into CDHWs as a new indicator (Perkins-Kirkpatrick and Lewis, 2020), the cumulative heat of CDHWs (DHC) was defined as the extra cumulative heat exceeding the heatwave threshold under drought conditions. This represents the sum of outliers between each heatwave day and the 90th percentile (Wang et al., 2022):

$$\mathrm{DHC}_{\mathrm{Ycum}} = \sum_{1}^{DHO} T_{\mathrm{anom}} \tag{1}$$

Where $\mathrm{DHC}_{\mathrm{Ycum}}$ represents the cumulative heat in a year, *DHO* represents the sum of all heatwave days in a year, and T_{anom} represents the temperature anomaly between all heatwave days and the heatwave threshold in a year.

Temperature anomalies of the yearly CDHWs (DHA) are defined as the average temperature anomalies of CDHWs, specifically defined as the cumulative heat of CDHWs in a year/total number of drought days in the year:

$$\mathrm{DHA}_{\mathrm{anom}} = \frac{\mathrm{DHC}_{\mathrm{Ycum}}}{drought} \tag{2}$$

Where $\mathrm{DHA}_{\mathrm{anom}}$ represents the average temperature anomaly of CDHWs in one year, and *drought* represents the total number of drought days in the year.

To compare these indicators with those of CDHWs, we calculated the compound wet-heatwave events (wet state [sc-PDSI>1]). We then judged whether there were significant differences among the CDHWs and compound wet-heatwave events indicators. Compound wet-heatwave events indicators correspond to CDHWs and are called WetDHF, WetDHD, WetDHO, WetDHM, WetDHC, and WetDHA.

Table 1
Definition of CDHW indicators.

Type	Short Name	Definition	Units
Frequency	DHF	Total frequency of CDHWs	event
Duration	DHD	Maximum duration of CDHWs in days	day
	DHO	Total occurrence days of CDHWs	day
Intensity	DHM	Average magnitude of yearly CDHWs	event yr^{-1}
	DHC	Cumulative heat of CDHWs	°C
	DHA	Temperature anomalies of yearly CDHWs	°C yr^{-1}

2.2.3. Statistical methods

In order to better explore the internal relationship between compound events, we applied three statistical methods. The first is Bayesian change point analysis (BCP), where the abrupt change point is the sudden change of parameters in the time series, characterized by any combination of parameters (Adams and MacKay, 2007; Barry and

Hartigan, 1993). We selected a univariate mutation point detection method, using it to obtain the probability of mutation of the corresponding mutation point. Specifically, the world is divided into arid regions and humid regions, and mutation points are detected for six indicators, respectively. Details on the mutation points, occurrence time and probability statistics can be found in Table S1. Detailed methodological explanations and formulas can be found in the methodology section of the supplementary material. The second statistical method we use here is Empirical Orthogonal Function (EOF) analysis. EOF can analyze spatio-temporal modal changes of CDHWs and structural features in matrix data and also extract the main data feature quantities (Wang et al., 2022). It decomposes the variable field that changes with time into a space function that does not change with time as well as a part that depends only on the time function. To simplify spatio-temporal datasets by transforming them into spatial modes of physical quantities and projecting them onto time, EOF has been widely used in meteorology, oceanography and hydrology (Braud and Obled, 1991; Zhu et al., 2021).

We defined 1961–1990 as the past period and 1991–2020 as the recent warm period (Jung and Schindler, 2022). Then we established the multiple linear regression model between CDHWs, sc-PDSI and heatwave, and the relative contributions of heatwaves and the sc-PDSI to CDHWs were respectively calculated by H. Wu et al. (2021) and X. Wu et al. (2020), as follows:

$$Y = a \times scPDSI + b \times Heatwave + c \tag{3}$$

Where Y represents the amount of change in CDHWs caused by drought and heatwave, a and b represent the regression coefficient, and c represents the constant.

Based on Eq. (3), the contribution and relative contribution of the sc-PDSI and heatwaves can be calculated as:

$$C_{scPDSI} = (a \times \Delta scPDSI)/\Delta CDHWs \tag{4}$$

$$C_{Heatwave} = (b \times \Delta Heatwave)/\Delta CDHWs \tag{5}$$

$$RC_{scPDSI} = |C_{scPDSI}| / (|C_{scPDSI}| + |C_{Heatwave}|) \tag{6}$$

$$RC_{Heatwave} = |C_{Heatwave}| / (|C_{scPDSI}| + |C_{Heatwave}|) \tag{7}$$

Where C_{scPDSI} and $C_{Heatwave}$ represent the contribution of drought and heatwave; $\Delta scPDSI$, $\Delta Heatwave$ and $\Delta CDHWs$ represent the average of drought index, heatwave index and CDHWs index variation in the first 30 years and the last 30 years, respectively, and RC_{scPDSI} and $RC_{Heatwave}$ represent the relative contributions of drought and heatwave to CDHWs.

The Granger Causality Test (GCT) is used to detect causality in time series, assessing whether one time series predicts changes in another based on a causal lag model. In a recent study, Green et al. (2017) analyzed the feedback between the biosphere and the atmosphere, which showed their regional differences. The stationarity of time series is the premise of GCT. Firstly, the stationarity and co-integration tests of time direction are carried out on grid points, one by one. Augmented Dickey-Fuller (ADF) is an effective method for testing the stationarity of time series (Gülen, 1996). The tested data can be analyzed using GCT (Fig. S2), establishing two regression models of stationary time series, which are assumed to be $X = \{x_t\}$ and $Y = \{y_t\}$:

$$y_t = \alpha + \sum_{t=1}^{n} \beta_t x_{t-1} + \sum_{t=1}^{n} \gamma_t y_{t-1} + \varepsilon_t \tag{8}$$

Where β_t is the trend item of time series data X, γ_t is the trend item of time series data Y, n is the maximum lag order of variables X and Y, α is a constant term, and ε_t represents the residual term.

In constructing the F statistic for the significance level test, the null hypothesis is that X is not the Granger cause that results in Y. If it passes the significance level test, the null hypothesis should be rejected, that is, X is the Granger cause that results in Y:

$$F = \frac{RS_R - RS_U}{RS_U} \times \frac{N-2n-1}{n} \sim F(n, N-2n-1) \tag{9}$$

Where RS_R is the sum of squares of the regression model established without considering X and when $\beta_t = 0$. RS_U is the sum of squares of the regression model established when X is considered and $\beta_t \neq 0$.

3. Results

3.1. Spatio-temporal variations of compound events in different regions

DHO represents an indicator of the duration of CDHWs, while DHC represents an indicator of the intensity of CDHWs. Fig. 2 shows the variability of CDHWs on a monthly scale. As can be seen, there is a sharp increase in both DHO and DHC month by month over the past 60 years (1961–2020), especially during the recent warm period (1991–2020), which nearly doubled compared to the past period (1961–1990). Further, there was an abrupt increase in DHO around 1997, and finding that DHO_drylands had the highest probability of mutation in 1997 at 0.706 by Bayesian mutation test (Table S1), which may be related to the shift in global temperature during this period, with a fluctuating increase in global temperature after 1980 and a jump between 1990 and 2000 (Hansen et al., 2006). There are no significant seasonal differences in DHO, but there are more anomalies in the last decade in particular, concentrated in summer and autumn. The DHC has more anomalies in the recent warm period in winter and spring compared to summer and autumn on a monthly scale, indicating a higher magnitude of heat accumulation in winter and spring.

CDHWs in drylands increased to varying degrees in time and space across the six assessed indicators for frequency, duration, and intensity (Fig. 3). The trend of spatial increase more pronounced in the drylands, where the rate of increase was nearly double that of the humid areas. The multi-year average intensity of CDHWs shows the same results (Figs. S3(a–f)), with the intensity of drylands generally stronger than that of humid areas. Meanwhile, the indicators of compound wet-heatwave events are higher on average in the humid areas than in the other areas, but still generally lower than the average intensity of CDHWs (Figs. S3(g–i)). The spatial areas where the frequency of CDHWs (DHF) increases significantly are basically in the drylands (Fig. 3(a)). Specifically, East Australia, Central Asia, North Africa and western Europe trends increase more significantly, reaching 0.12 events yr^{-1}, with arid and semi-arid areas showing greater variability with the wetter areas and globally.

Overall, CDHWs exhibit essentially the same regional increases in duration (DHD, DHO) (Fig. 3(b–c)). The regions where the total number of days of CDHWs occurred increased with a corresponding rise in their maximum duration. The same volatility is apparent in the time series variations. DHD and DHC show a significant increasing trend in the drylands and a slow decreasing trend in the humid areas. On the other hand, duration (DHM, DMC, DHA) indicators for CDHWs are relatively slow to increase regionally (Fig. 3(d–f)). Of these, DHM and DHA showed little regional variability, with DHA exhibiting stronger fluctuations and increasing trends in the humid areas, while DHC remained significantly different from the changes in the drylands and humid areas.

3.2. Differences between CDHWs and compound wet-heatwave events

Bayesian change point analysis (BCP) has been used for many years to detect mutations in CDHWs. In this study, Bayesian mutation point detection analysis was performed for CDHWs occurring in drylands and humid areas. The corresponding probability statistics are presented in Table S1. As can be seen in the table, the number of significant mutation points in the drylands was around 5 (probability value > 0.6) which is relatively small. Nonetheless, each indicator had a higher interannual growth rate compared to the humid areas (Figs. S4(a–f)). In contrast,

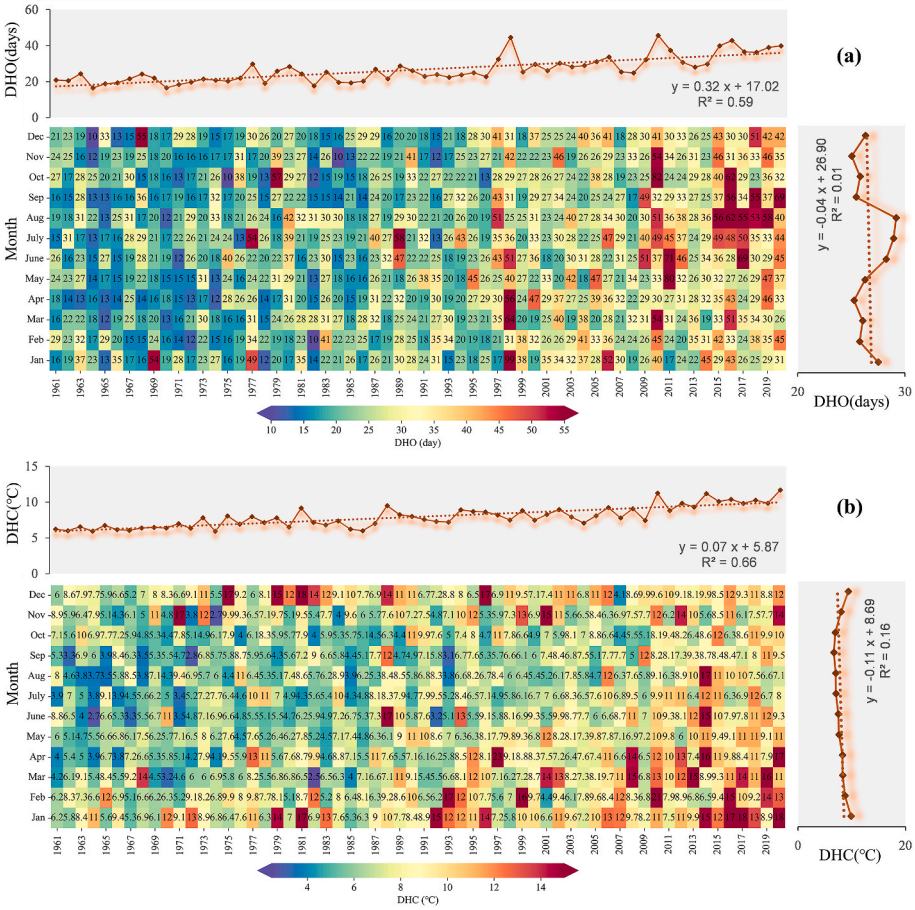

Fig. 2. Monthly and annual means of CDHWs are given on the panel axes (The brown curve represents the average over all years and all months on the top and right, respectively). (a) Global monthly-scale DHO distribution, (b) global monthly-scale DHC distribution. (For interpretation of the references to colour in this figure legend, the reader is referred to the Web version of this article.)

CDHWs in humid regions showed multi-variability, with mutation points in almost all indicators. Specifically, the total number of mutation points reached 11, more than double that of the drylands, with most of the mutation events occurring in the humid areas in DHF and DHO (Figs. S4(g–i)). CDHWs in the drylands have a large base and a faster growth rate, whereas in the humid areas, the fluctuation range is larger.

The multi-year mean of each indicator can be a good reflection of the state of the average distribution over the years. Accordingly, we calculated the difference between the multi-year mean of each indicator of CDHWs and compound wet-heatwave events (Fig. 4). As depicted in Fig. 4, the multi-year average intensities of the CDHW indicators are spatially stronger compared to the heatwave (sc-PDSI) indicators, which are nearly twice as intense and more pronounced in most drylands, particularly in Australia, South Africa and North America. The difference shows that most of the world is positive, with only the high latitudes of the northern hemisphere showing significant negative values, which may be related to the amplification effect of the Arctic. The arctic region has warmed almost four times faster than the rest of the world over the past four decades (Rantanen et al., 2022), exacerbating heatwave events.

We also found significant differences between CDHWs in drylands and humid areas, with non-significant differences for DHM and DHA indicators (Fig. 5(a–f)). Compound wet-heatwave events indicators are significantly different between drylands and humid areas and between drylands and globally (Figs. S5(a–f)). Further analysis of the intensity ratios between CDHW and compound wet-heatwave events metrics revealed that CDHWs were higher than compound wet-heatwave events in terms of frequency, intensity, and duration (Fig. 5(g–i)). At a global scale, the highest ratio of DHO intensity can be up to 2.04, with higher ratios for each indicator of CDHW in the drylands. In humid areas, however, the ratio of intensity between each indicator of CDHW and compound wet-heatwave events is > 1, with an intensity about 1.3 times higher. Table S2 presents the values of the ratios under each condition. As can be seen in the table, CDHWs are more frequent and more intense compared to compound wet-heatwave events in both drylands and humid region.

In the past (1961–1990) and recent (1991–2020) periods, 1990 and 2020 were selected as representative years to find the driest and hottest grid points occurring on a whole-year scale. Based on temporal directional ordering, and against all occurrences of drought, heatwaves, compound events and shifts in heatwave thresholds, it was found that there were significantly more compound events in representative years of both periods, particularly in April and November, and heatwave thresholds also increased by around 5 °C°(Fig. S6). Three indicators—DHF, DHD, and DHC—were selected to fit the kernel density of compound events occurring in drylands and humid areas during the base and control periods. CDHWs were found to occur in the past period at higher densities at lower frequencies, while the indicator values of CDHWs shifted towards higher values in the recent warm period. In other words, there was a significant increase in CDHWs during the transition phase from the past period to the recent warm period (Fig. 6).

3.3. *Dominant factors and compounding effects of CDHWs*

A multiple linear regression model was used to quantify the relative contribution of heatwave indicators and the sc-PDSI to CDHWs (Fig. 7

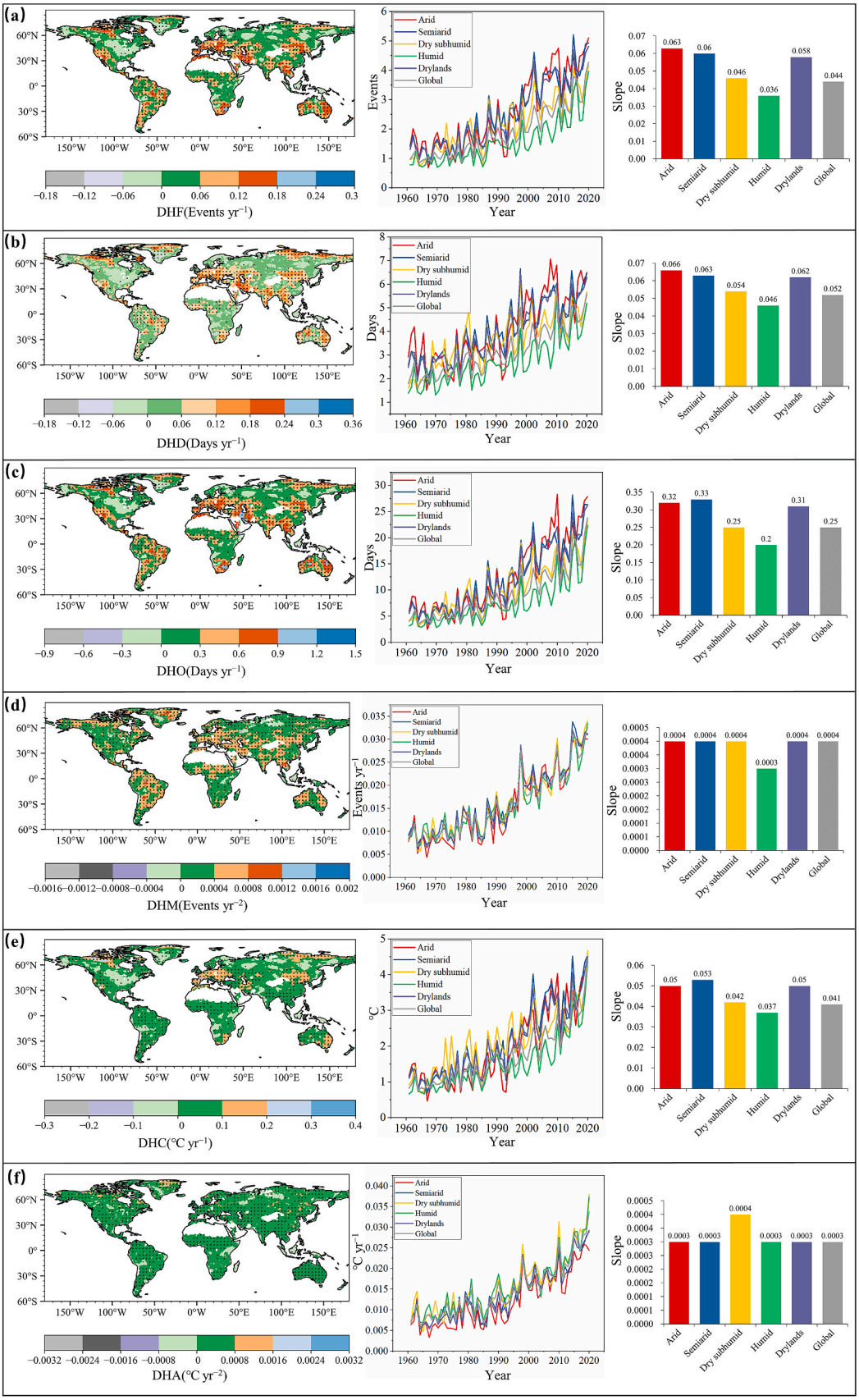

Fig. 3. (a–f) Spatial trend distribution of the six indicators of CDHWs and their time series variations in drylands and humid areas, divided by AI (black points highlight a 95% significance level).

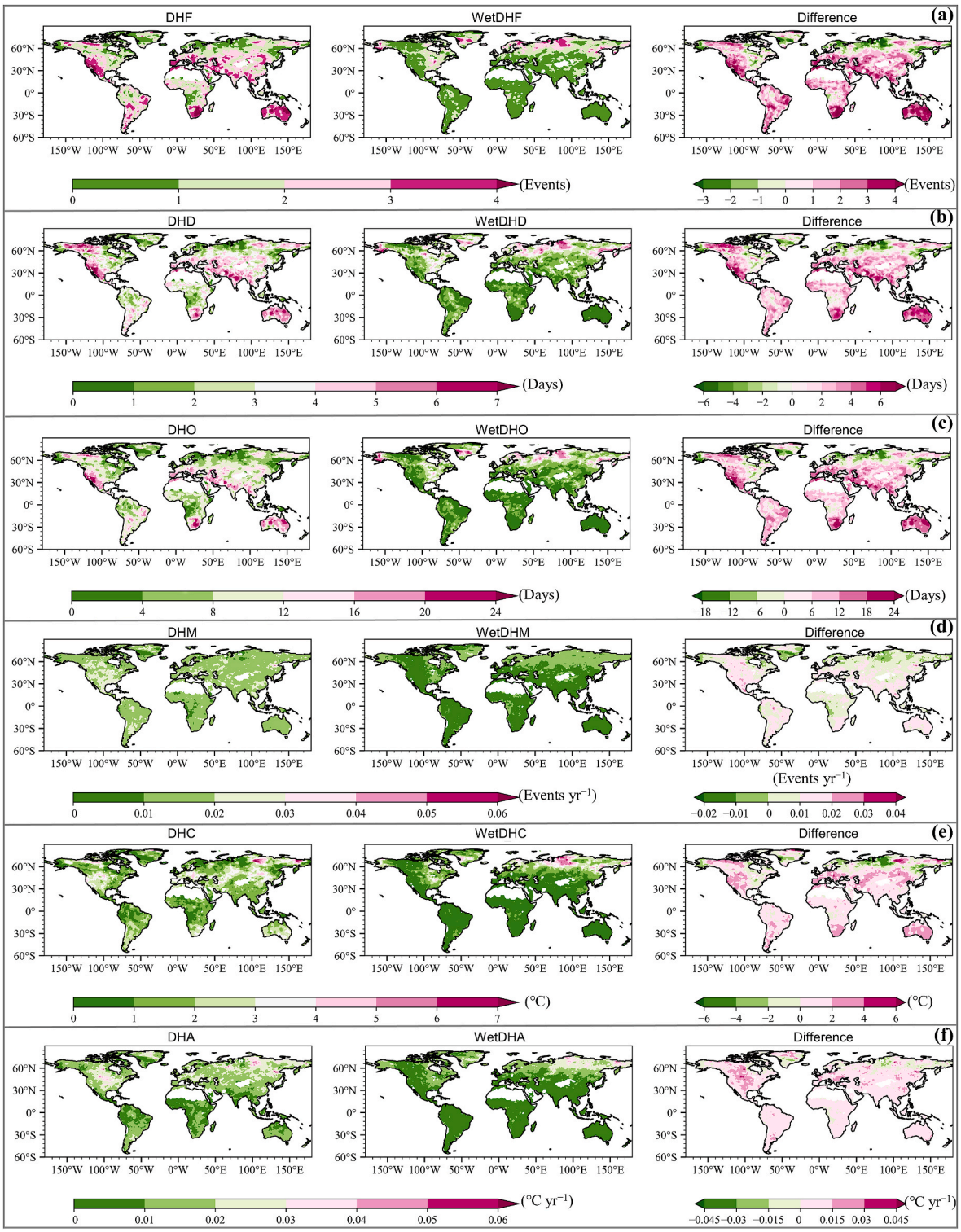

Fig. 4. Comparison of multi-year average differences between CDHWs and compound wet-heatwave events for each indicator (multi-year average of CDHW indicators subtracted from multi-year average of compound wet-heatwave events).

(a–d)). The relative contribution of heatwaves to CDHWs is high in drylands and significant in Central Asia, South America, Southern Africa and Australia, particularly in the Southern Africa and Australia drylands, where the relative contribution can reach more than 80%. Furthermore, it can be observed that in most drylands, the contribution of heatwaves to compound events is dominant, whereas in humid areas the opposite result is observed (Fig. 7(e–h)). The contribution of the droughts is high in Europe and northern Asia, with relative contributions of around 70% in most areas, which are largely in humid areas; the CDHWs in those areas are largely dominated by the droughts. It can also be demonstrated by the spatiotemporal correlation between sc-PDSI, heatwaves and CDHWs in drylands and humid areas. The correlation between compound events and heatwaves is higher in drylands than in humid areas, and can be on average about ten percentage points higher. At the same time, high density scatter is concentrated in areas of high values and occurs with greater intensity in arid areas (Figs. S7(a and c)).

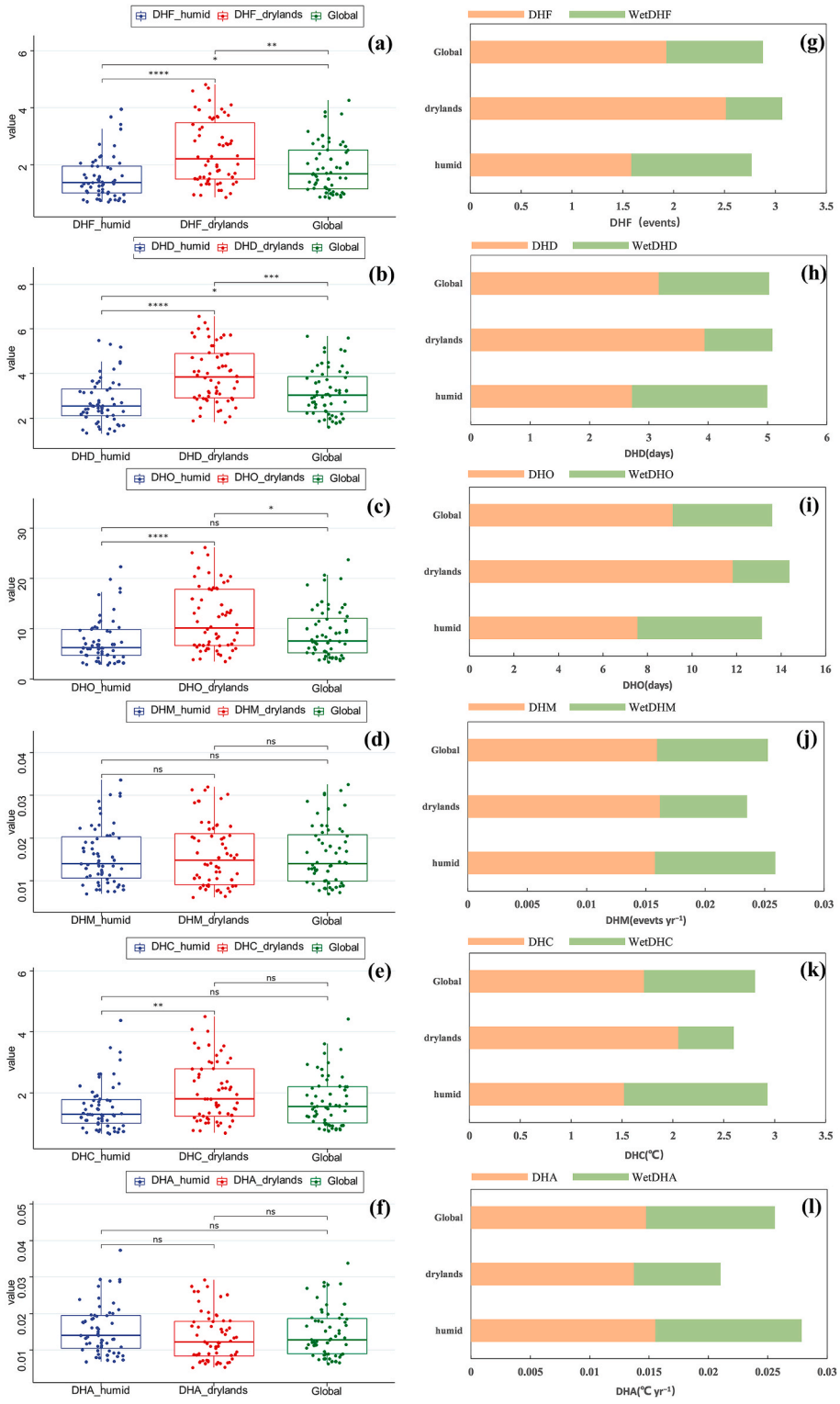

Fig. 5. (a–f) Distribution of each indicator of CDHWs in drylands and humid areas, showing whether there is a significant difference between them by *t*-test ("****, ***, **, * represent 0.1%, 1%, 5%, 10% significance levels, respectively), (g–i) Comparison of the mean intensity of CDHWs and compound wet-heatwave events in drylands and humid areas; detailed ratio values can be found in Table S2.

The spatial correlation between CDHWs and heatwaves is higher in drylands, especially in Australia, South Africa, North America and Central Asia, where the correlation coefficient can reach around 80% (Fig. S8). This demonstrates a higher correlation between the droughts and CDHWs in humid areas than in drylands (Figs. S7(b and d)). The degree of explanation for the correlation is about 15% higher in the drylands than in humid areas. In terms of spatial correlation, between the droughts and CDHWs the correlation is higher in humid areas, especially in Europe, northern Asia and North America, with a correlation coefficient of about 0.5 (Fig. S9).

The spatial mode can be analyzed for its contribution to the overall spatial field, and the temporal coefficients can be analyzed for the

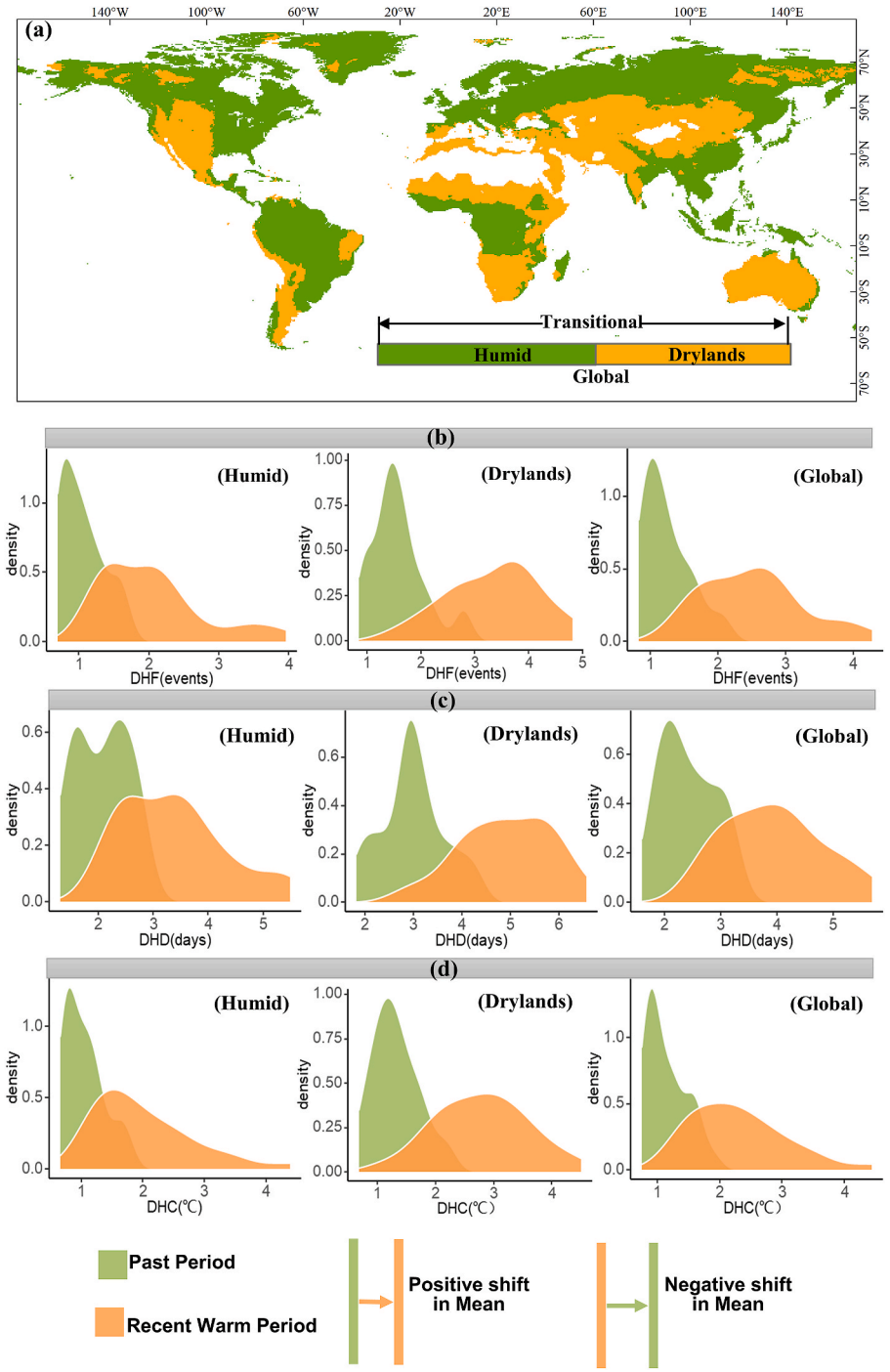

Fig. 6. Using 1961–1990 as the past period and 1991–2020 as the recent warm period, we studied the density shift characteristics of each indicator of CDHWs in the two periods for drylands and humid areas (transitional represents the shift of CDHWs in drylands or humid areas).

weight of the corresponding spatial contribution at a given epoch. We performed a multivariate EOF analysis of the normalised heatwave (days of occurrence, cumulative heat), droughts, and CDHWs (DHO, DHC) series. The cumulative variance contribution of the first three eigenvectors of the EOF amounts to about 30%, which basically reflects the modalities of the spatio-temporal distribution corresponding to those of heatwave, droughts and CDHWs. The modalities of the compound events were analyzed mainly on a monthly scale, with EOF1 and EOF2 of DHO reflecting the most severe DHO in regions with the most severe heatwave (days of occurrence), droughts and the longest heatwave, and vice versa.

Figs. S10(a–b) EOF3 shows heatwave (days of occurrence) and the sc-PDSI in areas with the most severe droughts and longest days of heatwave occurrence, but relatively little DHO occurrence (Fig. S10c). The EOF1 and EOF3 of the DHC reflect the lower cumulative heat of CDHWs in the regions where heatwave (cumulative heat) droughts is most severe and is the dominant spatial distribution pattern (Figs. S11(a and c)). In contrast, EOF2 reflects the higher accumulation of heat in CDHWs in areas where heatwave (cumulative heat), droughts is most severe, corresponding to the dominant spatial distribution pattern of DHO (Fig. S11b). The results show that the time coefficients of DHO and DHC are generally more positive than negative in part and contribute positively to the spatial field, and there is a good positive correspondence between CDHWs, droughts, and heatwaves.

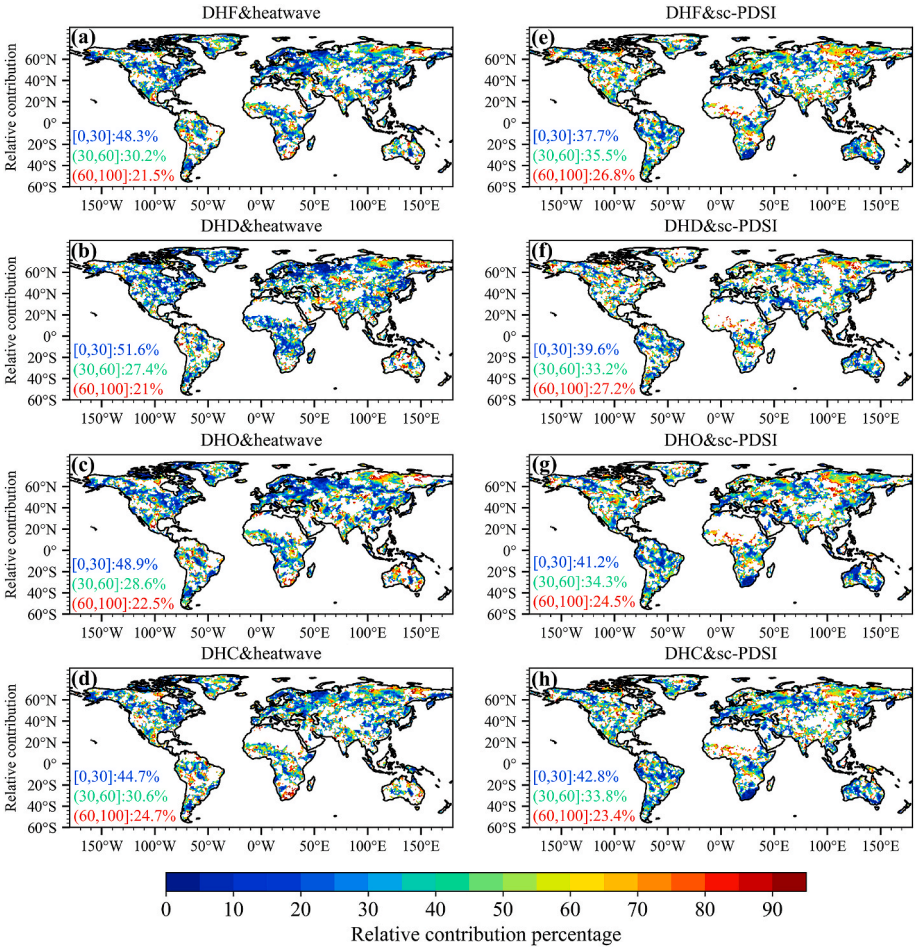

Fig. 7. Relative contributions of each index of heatwave and drought to CDHWs were established using the multiple linear regression model. The relative contributions were counted for each raster in [0,30], (30,60), and [60,100] percentile intervals, respectively, as a proportion of the total raster. (For interpretation of the references to colour in this figure legend, the reader is referred to the Web version of this article.)

In considering the optimal lag (Fig. S12), we analyzed the Granger causality of the droughts and heatwaves on CDHWs (Fig. 8). The results show strong spatial correlations and compounding effects. At the 0.1 significance level, 39.1% (DHO&heatwave) of the heatwave and 45.8% (DHD&sc-PDSI) of the droughts for CDHWs can be explained by the Granger test using the BEST model, with a higher percentage of explanatory power in the drylands compared to humid areas (Table S3). Furthermore, the spatial distribution of Granger causality of the droughts and heatwaves on CDHWs has the same spatial distribution characteristics in Australia, South Africa, North America, Central Asia and Northern Asia. This indicates that the Granger causality of the droughts and heatwaves on CDHWs is strongly spatially correlated and compounding effects in these drylands.

Granger's optimal lagging results remain largely unchanged at around 3 years, with most regions having a lagging effect of 1–2 years. In general, the lagging effect of heatwaves is longer than the lagging effect of the droughts, particularly in Australia, Europe, South America and northern Asia. Additionally, the lagged years of heatwaves are longer in most drylands, while the lag of the droughts is longer in most humid areas compared to drylands (Fig. S12).

4. Discussion

This study focuses on the intensity changes of CDHWs and compound wet-heatwave events and their evolution patterns under different dry and wet conditions on a global scale from 1961 to 2020, and analyzes the intensity differences between the two in depth, with a special focus on the relative contributions of droughts and heatwaves to CDHWs and their compounding effects in different drylands and humid areas, and the study provides new insights into CDHWs. The results of CDHWs calculated in this paper using CPC data and Berkeley data are in high consistency (Fig. S13). We found that CDHWs increased twice as much as compound wet-heatwave events, and that the frequency of CDHWs was concentrated in Australia, India, southern Africa and western North America, which is consistent with previous studies (Bevacqua et al., 2022; Fan et al., 2022; Wu et al., 2020b). The difference is that compound wet-heatwave events are mainly concentrated in northern Asia. In addition, the relative contributions of drought and heatwaves have more similar spatial distribution patterns, especially in the drylands where the contributions are higher (Wu et al., 2021). It was found that the relative contribution of heatwaves to CDHWs dominates in the drylands, due to the high regional variability of heatwaves (Liang et al., 2022; Perkins-Kirkpatrick and Lewis, 2020). Warming is greater in the drylands than in the humid areas (Li et al., 2017), often leads to more frequent heatwaves in drylands. Based on Coupled Model Intercomparison Project Phase 6 (CMIP6) data model simulations, CDHWs will continue to increase in frequency and intensity through the end of the 21st century, with approximately 20% of the global land area exposed to CDHWs lasting up to 25 days per year (De Luca and Donat, 2023; Tripathy et al., 2023).

Geographic location, climatic characteristics, and surface conditions influence the different manifestations of droughts, heatwaves, and CDHWs, including temperature, precipitation, and soil properties (Lian et al., 2021). Tmax in the drylands was twice as high as in the humid

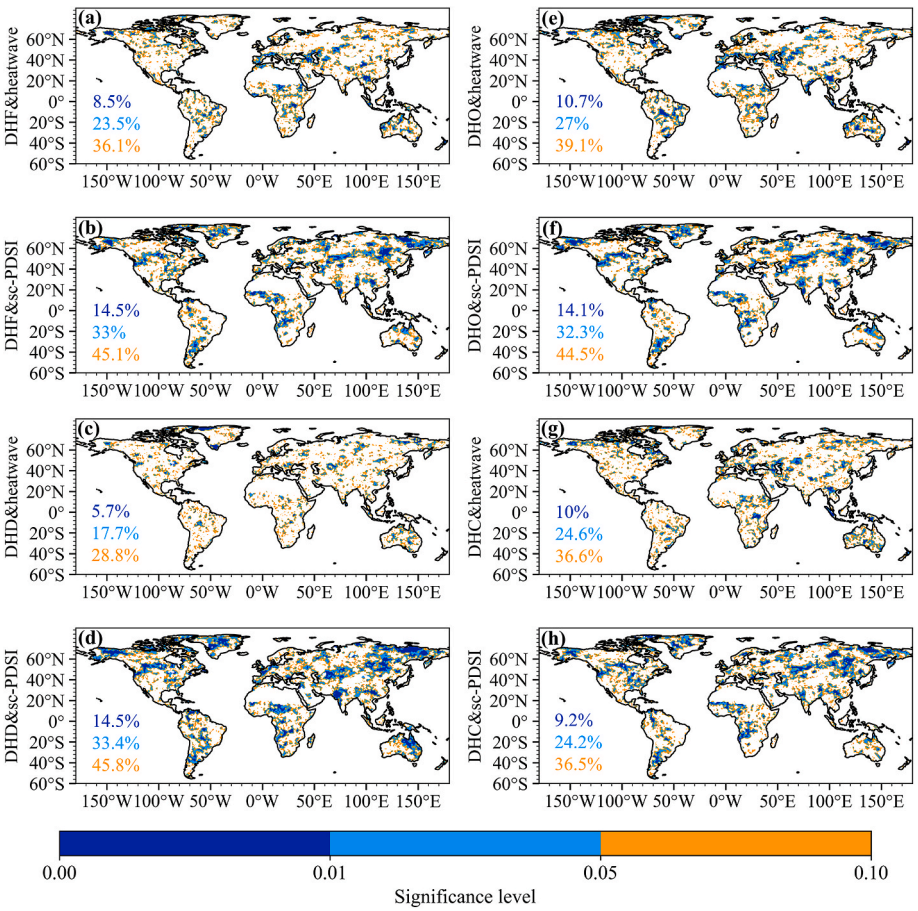

Fig. 8. Results of Granger causality test between droughts, heatwaves and CDHWs, with the percentages calculated at different significance levels.

areas (Fig. S14). The intensity of occurrence of CDHWs was higher in the drylands than in the humid areas. Droughts occurring in drylands are often characterized by prolonged and intense droughts (Berg and McColl, 2021), when combined with heatwaves, may further lead to more severe drought conditions (Li et al., 2021). Heatwaves in the humid areas are often characterized by high humidity, which can lead to extreme heat in the short term, posing a threat to human health and ecosystems (Chen et al., 2022). CDHWs can lead to more extreme and prolonged high temperatures and droughts with severe agricultural, ecological and socio-economic impacts (Zscheischler et al., 2020). It has been found that the humid areas cumulates more heat than the drylands, which gradually raises the threshold for the occurrence of heatwaves in the humid areas, leading to the occurrence of more intense heatwaves. We find that heatwave thresholds increased by about 5 °C from 1961 to 2020. Understanding these differences and the factors influencing them can help to better respond to droughts, heatwaves and CDHWs in different areas. Targeted coping strategies and policies are developed to mitigate their adverse ecological and human social impacts (Hao and Singh, 2020; Zscheischler et al., 2020).

The reasons for this variability are complex and varied, including threshold selection, model differences (process-based or statistical models), spatial and temporal scales of the data, methodological selection of CDHWs, and drought indicator definitions (Hao and Singh, 2020). Uncertainty in mean precipitation trends is strongly modulated by large-scale atmospheric circulation (Green et al., 2017). The significance of precipitation trends may determine the occurrence of future CDHWs, and changes in CDHWs depend on models, regional characteristics, and internal climate variability (Bevacqua et al., 2022). Drought indices tend to have more room for choice, depending mainly on the measure, applied to meteorological drought or hydrological drought, Standardized Precipitation Index (SPI), Standardized Precipitation Evapotranspiration Index (SPEI), sc-PDSI, Standardized Runoff Index (SRI), etc., have been studied, and are mainly different for the selection of the study object (De Luca and Donat, 2023; Mukherjee and Mishra, 2021; Yin et al., 2022). Sensitivity of sc-PDSI to critical thresholds defining drought and wet conditions found that drought (sc-PDSI $= -1$) was more sensitive compared to the wet threshold (sc-PDSI $= 1$), with drought critical thresholds exhibiting higher percentile distributions such as in southern Africa and Australia (Fig. S15). An in-depth investigation of these differences can reduce uncertainty and enhance knowledge about CDHWs.

The occurrence of CDHWs is often driven by climatic conditions with multivariate influences, which in turn result in spatial compounds, and analyzing the uncertainty of the influencing factors that contribute to this phenomenon will help us to better cope with extreme climate events (Zscheischler et al., 2020). Droughts, heatwaves or CDHWs are often triggered by anticyclonic flow patterns, which in turn are limited by various surface fluxes (Mitchell et al., 2016), and can result in different spatial patterns regionally due to temperature and precipitation anomalies (Konapala et al., 2020). Multivariate dependence is closely related to the likelihood of CDHWs occurring, and changes in atmospheric circulation or terrestrial air feedbacks in the context of global warming may lead to changes in the structure of multivariate dependence of CDHWs, increasing the risk of ecological or economic and social impacts of CDHWs (Hao and Singh, 2020). Elevated summer VPD will exacerbate drought events, warmer temperatures will increase the occurrence of hotter droughts, and heatwaves will become more frequent (Gazol and Julio Camarero, 2022). Exacerbation of soil drought and atmospheric drought may lead to an increase in snow drought (Snow drought is a period of unusually low snowpack for the time of year) events, which

further contributes to an increase in heatwave events (Li and Wang, 2022). The impact of human activities on the occurrence of CDHWs is not negligible (Chen et al., 2022; Mukherjee and Mishra, 2021). Urbanization and human activities have been found to significantly increase the incidence of extreme summer heat in China, so the impact of anthropogenic factors on heatwaves and droughts cannot be underestimated (Zhang et al., 2021). In addition, we found that CDHWs tend to cumulate higher heat in winter and spring. Possibly due to anomalously high surface temperatures and frequent droughts, the impact of CDHWs on ecosystems in winter and spring is a topic of concern (Yin et al., 2022, 2023).

There is an urgent need to enhance multi-model integration in the future to deepen the understanding of CDHWs and provide new opportunities for climate change mitigation (Bevacqua et al., 2022). We should fully consider the regional characteristics of drylands and humid areas and scientifically select different disaster factors in order to deeply study the physical mechanisms within these areas, especially the formation mechanism of CDHWs in drylands and humid areas. There is also a need to strengthen the capacity to respond to the adverse impacts of CDHWs on agriculture, ecology and public health. Research on CDHWs provides substantial support to policy makers in addressing climate change and deserves the full support and attention of countries and relevant sectors.

5. Conclusions

(1) CDHWs have generally increased in global spatial and temporal trends, with the rate and average intensity of increase in drylands nearly double the increase in humid areas. CDHWs have increased significantly in the recent warm period (1991–2020) compared to the past period (1961–2020), with no significant seasonal differences in DHO. However, more anomalies have appeared in the last decade. Specifically, DHC has more anomalies in the recent warm period as well as a higher magnitude of heat accumulation in winter and spring.

(2) The multi-year average intensity of each indicator of CDHWs is spatially stronger compared to the multi-year average intensity of each indicator of compound wey-heatwave events, which is nearly twice as intense and more pronounced in most drylands, especially in Australia, South Africa and North America. Intensities were around 1.3 times higher, indicating that CDHWs are more frequent and more intense compared to compound wet-heatwave events in both drylands and humid areas.

(3) Heatwave (cumulative heat), sc-PDSI is most severe in regions where CDHWs are also more severe, which is the dominant spatial distribution pattern. Furthermore, the relative contribution of heatwaves to CDHWs is higher in most drylands, particularly in Southern Africa as well as the Australian drylands. The relative contribution of the droughts to CDHWs is higher in most of the humid areas, with a relative contribution of around 70%. There was a strong spatial correlation and compounding effects of droughts, heatwave and CDHWs, taking into account the optimal lag. At the 0.1 significance level, 39.1% (DHO&heatwave) of heatwave and 45.8% (DHD&sc-PDSI) of droughts on CDHWs can be explained by the Granger test, with a higher percentage of explanatory power in the drylands compared to the humid areas.

CRediT authorship contribution statement

Chuan Wang: Conceptualization, Methodology, Software, Validation, Writing – original draft, Writing – review & editing. **Zhi Li:** Conceptualization, Funding acquisition, Writing – review & editing. **Yaning Chen:** Conceptualization. **Lin Ouyang:** Software. **Yupeng Li:** Software. **Fan Sun:** Validation. **Yongchang Liu:** Validation. **Jianyu Zhu:** Writing – review & editing.

Declaration of competing interest

The authors declare that they have no known competing financial interests or personal relationships that could have appeared to influence the work reported in this paper.

Data availability

Our results data for this paper: https://zenodo.org/record/7230778#.Y1F5xXZBztV.

Acknowledgements

The research is supported by the National Key Research and Development Program (2019YFA0606902) and the National Natural Science Foundation of China (U2003302). The authors gratefully acknowledge the Youth Innovation Promotion Association of the Chinese Academy of Sciences (Y2022108).

We thank the editors and reviewers for their constructive comments and the Centre for Climate Research (CRU), the Berkeley Earth Surface Temperature Project, and the Climate Prediction Center (CPC) for providing the data.

Appendix A. Supplementary data

Supplementary data to this article can be found online at https://doi.org/10.1016/j.wace.2023.100632.

References

Adams, R.P., MacKay, D.J.C., 2007. Bayesian Online Changepoint Detection. https://doi.org/10.48550/arXiv.0710.3742.

An, L., Wang, J., Huang, J., Pokhrel, Y., Hugonnet, R., Wada, Y., Cáceres, D., Müller Schmied, H., Song, C., Berthier, E., Yu, H., Zhang, G., 2021. Divergent causes of terrestrial water storage decline between drylands and humid regions globally. Geophys. Res. Lett. 48 https://doi.org/10.1029/2021GL095035.

Baltas, E., 2007. Spatial distribution of climatic indices in northern Greece. Meteorol. Appl. 14, 69–78. https://doi.org/10.1002/met.7.

Barichivich, J., Osborn, T., Harris, I., van der Schrier, G., Jones, P., 2019. Drought: monitoring global drought using the self-calibrating palmer drought severity index. Bull. Am. Meteorol. Soc. 100, S39–S40. https://doi.org/10.1175/2019BAMSStateoftheClimate.1.

Barry, D., Hartigan, J.A., 1993. A bayesian analysis for change point problems. J. Am. Stat. Assoc. 88, 309–319. https://doi.org/10.1080/01621459.1993.10594323.

Berg, A., McColl, K.A., 2021. No projected global drylands expansion under greenhouse warming. Nat. Clim. Change 11, 331–337. https://doi.org/10.1038/s41558-021-01007-8.

Bevacqua, E., Zappa, G., Lehner, F., Zscheischler, J., 2022. Precipitation trends determine future occurrences of compound hot–dry events. Nat. Clim. Change 12, 350–355. https://doi.org/10.1038/s41558-022-01309-5.

Brás, T.A., Seixas, J., Carvalhais, N., Jägermeyr, J., 2021. Severity of drought and heatwave crop losses tripled over the last five decades in Europe. Environ. Res. Lett. 16 https://doi.org/10.1088/1748-9326/abf004.

Braud, I., Obled, Ch, 1991. On the use of Empirical Orthogonal Function (EOF) analysis in the simulation of random fields. Stoch. Hydrol. Hydraul. 5, 125–134. https://doi.org/10.1007/BF01543054.

Chen, H., Zhao, L., Dong, W., Cheng, L., Cai, W., Yang, J., Bao, J., Liang, X.-Z., Hajat, S., Gong, P., Liang, W., Huang, C., 2022. Spatiotemporal variation of mortality burden attributable to heatwaves in China, 1979–2020. Sci. Bull. 67, 1340–1344. https://doi.org/10.1016/j.scib.2022.05.006.

De Luca, P., Donat, M.G., 2023. Projected changes in hot, dry, and compound hot-dry extremes over global land regions. Geophys. Res. Lett. 50, e2022GL102493 https://doi.org/10.1029/2022GL102493.

Domeisen, D.I.V., Eltahir, E.A.B., Fischer, E.M., Knutti, R., Perkins-Kirkpatrick, S.E., Schär, C., Seneviratne, S.I., Weisheimer, A., Wernli, H., 2022. Prediction and projection of heatwaves. Nat. Rev. Earth Environ. 4, 36–50. https://doi.org/10.1038/s43017-022-00371-z.

Fan, L.-J., Yan, Z.-W., Chen, D., Li, Z., 2022. Assessment of Central Asian heat extremes by statistical downscaling: Validation and future projection for 2015–2100. Adv. Clim. Change Res. 13, 14–27. https://doi.org/10.1016/j.accre.2021.09.007.

Feng, S., Hao, Z., Zhang, X., Hao, F., 2019. Probabilistic evaluation of the impact of compound dry-hot events on global maize yields. Sci. Total Environ. 689, 1228–1234. https://doi.org/10.1016/j.scitotenv.2019.06.373.

Gazol, A., Julio Camarero, J., 2022. Compound climate events increase tree drought mortality across European forests. Sci. Total Environ. 816 https://doi.org/10.1016/j.scitotenv.2021.151604.

Green, J.K., Konings, A.G., Alemohammad, S.H., Berry, J., Entekhabi, D., Kolassa, J., Lee, J.-E., Gentine, P., 2017. Regionally strong feedbacks between the atmosphere and terrestrial biosphere. Nat. Geosci. 10, 410–414. https://doi.org/10.1038/ngeo2957.
Gülen, S.G., 1996. Is OPEC a cartel? Evidence from cointegration and causality tests. Energy J. 17, 43–57.
Hansen, J., Sato, M., Ruedy, R., Lo, K., Lea, D.W., Medina-Elizade, M., 2006. Global temperature change. Proc. Natl. Acad. Sci. USA 103, 14288–14293. https://doi.org/10.1073/pnas.0606291103.
Hao, Z., 2022. Compound events and associated impacts in China. iScience 25, 104689. https://doi.org/10.1016/j.isci.2022.104689.
Hao, Z., Singh, V.P., 2020. Compound events under global warming: a dependence perspective. J. Hydrol. Eng. 25, 03120001 https://doi.org/10.1061/(ASCE)HE.1943-5584.0001991.
Harris, I., Osborn, T.J., Jones, P., Lister, D., 2020. Version 4 of the CRU TS monthly high-resolution gridded multivariate climate dataset. Sci. Data 7, 109. https://doi.org/10.1038/s41597-020-0453-3.
Hoover, D.L., Hajek, O.L., Smith, M.D., Wilkins, K., Slette, I.J., Knapp, A.K., 2022. Compound hydroclimatic extremes in a semi-arid grassland: drought, deluge, and the carbon cycle. Global Change Biol. 28, 2611–2621. https://doi.org/10.1111/gcb.16081.
Huang, J., Ji, M., Xie, Y., Wang, S., He, Y., Ran, J., 2016. Global semi-arid climate change over last 60 years. Clim. Dynam. 46, 1131–1150. https://doi.org/10.1007/s00382-015-2636-8.
Jung, C., Schindler, D., 2022. A review of recent studies on wind resource projections under climate change. Renew. Sustain. Energy Rev. 165, 112596 https://doi.org/10.1016/j.rser.2022.112596.
Konapala, G., Mishra, A.K., Wada, Y., Mann, M.E., 2020. Climate change will affect global water availability through compounding changes in seasonal precipitation and evaporation. Nat. Commun. 11, 3044. https://doi.org/10.1038/s41467-020-16757-w.
Le, M.-H., Dinh, K.V., Nguyen, M.V., Rønnestad, I., 2020. Combined effects of a simulated marine heatwave and an algal toxin on a tropical marine aquaculture fish cobia (Rachycentron canadum). Aquacult. Res. 51, 2535–2544. https://doi.org/10.1111/are.14596.
Li, J., Tam, C.-Y., Tai, A.P.K., Lau, N.-C., 2021. Vegetation-heatwave correlations and contrasting energy exchange responses of different vegetation types to summer heatwaves in the Northern Hemisphere during the 1982-2011 period. Agric. For. Meteorol. 296, 108208 https://doi.org/10.1016/j.agrformet.2020.108208.
Li, X., Wang, S., 2022. Recent increase in the occurrence of snow droughts followed by extreme heatwaves in a warmer world. Geophys. Res. Lett. 49 https://doi.org/10.1029/2022GL099925.
Li, Y., Chen, Y., Li, Z., 2019. Dry/wet pattern changes in global dryland areas over the past six decades. Global Planet. Change 178, 184–192. https://doi.org/10.1016/j.gloplacha.2019.04.017.
Li, Z., Chen, Y., Fang, G., Li, Y., 2017. Multivariate assessment and attribution of droughts in Central Asia. Sci. Rep. 7, 1316. https://doi.org/10.1038/s41598-017-01473-1.
Lian, X., Piao, S., Chen, A., Huntingford, C., Fu, B., Li, L.Z.X., Huang, J., Sheffield, J., Berg, A.M., Keenan, T.F., McVicar, T.R., Wada, Y., Wang, X., Wang, T., Yang, Y., Roderick, M.L., 2021. Multifaceted characteristics of dryland aridity changes in a warming world. Nat. Rev. Earth Environ. 2, 232–250. https://doi.org/10.1038/s43017-021-00144-0.
Liang, L., Yu, L., Wang, Z., 2022. Identifying the dominant impact factors and their contributions to heatwave events over mainland China. Sci. Total Environ. 848, 157527 https://doi.org/10.1016/j.scitotenv.2022.157527.
Maule, C.F., Thejll, P., Christensen, J.H., Svendsen, S.H., Hannaford, J., 2013. Improved confidence in regional climate model simulations of precipitation evaluated using drought statistics from the ENSEMBLES models. Clim. Dynam. 40, 155–173. https://doi.org/10.1007/s00382-012-1355-7.
Mitchell, D., Heaviside, C., Vardoulakis, S., Huntingford, C., Masato, G., P Guillod, B., Frumhoff, P., Bowery, A., Wallom, D., Allen, M., 2016. Attributing human mortality during extreme heat waves to anthropogenic climate change. Environ. Res. Lett. 11, 074006 https://doi.org/10.1088/1748-9326/11/7/074006.
Mukherjee, S., Mishra, A.K., 2021. Increase in compound drought and heatwaves in a warming world. Geophys. Res. Lett. 48 https://doi.org/10.1029/2020GL090617.
Mukherjee, S., Mishra, A.K., Ashfaq, M., Kao, S.-C., 2022. Relative effect of anthropogenic warming and natural climate variability to changes in Compound drought and heatwaves. J. Hydrol. 605, 127396 https://doi.org/10.1016/j.jhydrol.2021.127396.
Perkins-Kirkpatrick, S.E., Lewis, S.C., 2020. Increasing trends in regional heatwaves. Nat. Commun. 11, 3357. https://doi.org/10.1038/s41467-020-16970-7.
Pyrgou, A., Hadjinicolaou, P., Santamouris, M., 2020. Urban-rural moisture contrast: regulator of the urban heat island and heatwaves' synergy over a mediterranean city. Environ. Res. 182, 109102 https://doi.org/10.1016/j.envres.2019.109102.
Rantanen, M., Karpechko, A.Y., Lipponen, A., Nordling, K., Hyvärinen, O., Ruosteenoja, K., Vihma, T., Laaksonen, A., 2022. The Arctic has warmed nearly four times faster than the globe since 1979. Commun. Earth Environ. 3, 1–10. https://doi.org/10.1038/s43247-022-00498-3.
Reddy, P.J., Perkins-Kirkpatrick, S.E., Ridder, N.N., Sharples, J.J., 2022. Combined role of ENSO and IOD on compound drought and heatwaves in Australia using two CMIP6 large ensembles. Weather Clim. Extrem. 37 https://doi.org/10.1016/j.wace.2022.100469.
Ridder, N.N., Pitman, A.J., Ukkola, A.M., 2022. High Impact Compound Events in Australia, vol. 36. WEATHER Clim. https://doi.org/10.1016/j.wace.2022.100457. Extrem.
Rohde, R.A., Hausfather, Z., 2020. The Berkeley Earth land/ocean temperature record. Earth Syst. Sci. Data 12, 3469–3479. https://doi.org/10.5194/essd-12-3469-2020.
Shi, Z., Jia, G., Zhou, Y., Xu, X., Jiang, Y., 2021. Amplified intensity and duration of heatwaves by concurrent droughts in China. Atmos. Res. 261 https://doi.org/10.1016/j.atmosres.2021.105743.
Sutanto, S.J., Vitolo, C., Di Napoli, C., D'Andrea, M., Van Lanen, H.A.J., 2020. Heatwaves, droughts, and fires: exploring compound and cascading dry hazards at the pan-European scale. Environ. Int. 134 https://doi.org/10.1016/j.envint.2019.105276.
Tripathy, K.P., Mukherjee, S., Mishra, A.K., Mann, M.E., Williams, A.P., 2023. Climate change will accelerate the high-end risk of compound drought and heatwave events. Proc. Natl. Acad. Sci. USA 120, e2219825120. https://doi.org/10.1073/pnas.2219825120.
Wang, C., Li, Z., Chen, Y., Li, Y., Liu, X., Hou, Y., Wang, X., Kulaixi, Z., Sun, F., 2022. Increased compound droughts and heatwaves in a double pack in central Asia. Rem. Sens. 14, 2959. https://doi.org/10.3390/rs14132959.
Wells, N., Goddard, S., Hayes, M.J., 2004. A self-calibrating palmer drought severity index. J. Clim. 17, 2335–2351. https://doi.org/10.1175/1520-0442(2004)017<2335:ASPDSI>2.0.CO;2.
Wu, H., Su, X., Singh, V.P., 2021. Blended dry and hot events index for monitoring dry-hot events over global land areas. Geophys. Res. Lett. 48, e2021GL096181 https://doi.org/10.1029/2021GL096181.
Wu, X., Hao, Z., Zhang, X., Li, C., Hao, F., 2020a. Evaluation of severity changes of compound dry and hot events in China based on a multivariate multi-index approach. J. Hydrol. 583, 124580 https://doi.org/10.1016/j.jhydrol.2020.124580.
Wu, X., Hao, Z., Zhang, X., Li, C., Hao, F., 2020b. Based on a multivariate multi-index approach. J. Hydrol. 9.
Xu, C., McDowell, N.G., Fisher, R.A., Wei, L., Sevanto, S., Christoffersen, B.O., Weng, E., Middleton, R.S., 2019. Increasing impacts of extreme droughts on vegetation productivity under climate change. Nat. Clim. Change 9, 948–953. https://doi.org/10.1038/s41558-019-0630-6.
Yin, J., Gentine, P., Slater, L., Gu, L., Pokhrel, Y., Hanasaki, N., Guo, S., Xiong, L., Schlenker, W., 2023. Future socio-ecosystem productivity threatened by compound drought–heatwave events. Nat. Sustain. 6, 259–272. https://doi.org/10.1038/s41893-022-01024-1.
Yin, J., Slater, L., Gu, L., Liao, Z., Guo, S., Gentine, P., 2022. Global increases in lethal compound heat stress: hydrological drought hazards under climate change. Geophys. Res. Lett. 49 https://doi.org/10.1029/2022GL100880.
Zhang, W., Luo, M., Gao, S., Chen, W., Hari, V., Khouakhi, A., 2021. Compound hydrometeorological extremes: drivers, mechanisms and methods. Front. Earth Sci. 9, 673495 https://doi.org/10.3389/feart.2021.673495.
Zhang, Y., Hao, Z., Feng, S., Zhang, X., Hao, F., 2022. Changes and driving factors of compound agricultural droughts and hot events in eastern China. Agric. Water Manag. 263, 107485 https://doi.org/10.1016/j.agwat.2022.107485.
Zhou, S., Yuan, X., 2022. Upwind droughts enhance half of the heatwaves over North China. Geophys. Res. Lett. 49 https://doi.org/10.1029/2021GL096639.
Zhou, S., Zhang, Y., Park Williams, A., Gentine, P., 2019. Projected increases in intensity, frequency, and terrestrial carbon costs of compound drought and aridity events. Sci. Adv. 5 https://doi.org/10.1126/sciadv.aau5740 eaau5740.
Zhu, Y., Liu, S.Y., Yi, Y., Xie, F.M., Grunwald, R., Miao, W.F., Wu, K.P., Qi, M.M., Gao, Y. P., Singh, D., 2021. Overview of terrestrial water storage changes over the Indus River Basin based on GRACE/GRACE-FO solutions. Sci. Total Environ. 799 https://doi.org/10.1016/j.scitotenv.2021.149366.
Zscheischler, J., Martius, O., Westra, S., Bevacqua, E., Raymond, C., Horton, R.M., van den Hurk, B., AghaKouchak, A., Jézéquel, A., Mahecha, M.D., Maraun, D., Ramos, A. M., Ridder, N.N., Thiery, W., Vignotto, E., 2020. A typology of compound weather and climate events. Nat. Rev. Earth Environ. 1, 333–347. https://doi.org/10.1038/s43017-020-0060-z.
Zscheischler, J., Westra, S., van den Hurk, B.J.J.M., Seneviratne, S.I., Ward, P.J., Pitman, A., AghaKouchak, A., Bresch, D.N., Leonard, M., Wahl, T., Zhang, X., 2018. Future climate risk from compound events. Nat. Clim. Change 8, 469–477. https://doi.org/10.1038/s41558-018-0156-3.